analytical chemistry
Article
pubs.acs.org/ac

Partnering Analytic Models and Dynamic Secondary Ion Mass Spectrometry Simulations to Interpret Depth Profiles Due to Kiloelectronvolt Cluster Bombardment

Robert J. Paruch,[†] Barbara J. Garrison,*[,‡] and Zbigniew Postawa*[,†]

[†]Smoluchowski Institute of Physics, Jagiellonian University, ul. Reymonta 4, 30-059 Kraków, Poland

[‡]Department of Chemistry, 104 Chemistry Building, Penn State University, University Park, Pennsylvania 16802, United States

ABSTRACT: The analytical steady-state statistical sputtering model (SS-SSM) is utilized to interpret molecular dynamics (MD) simulations of depth profiling of Ag solids with keV cluster beams of C_{60} and Au_3 under different incident energy and angle conditions. Specifically, the results of the MD simulations provide the input to the SS-SSM and the result is a depth profile of a delta layer. It has been found that the rms roughness of each system correlates with the total displacement yield, a new quantity introduced in this study that follows naturally from the SS-SSM. The results indicate that the best depth profiles occur when the displacement yield is low and the sputtering yield is high. Moreover, it is determined that the expected value of the delta layer position as calculated from a depth profile rather than the peak position in the depth profile is the best indicator of the actual delta layer position.

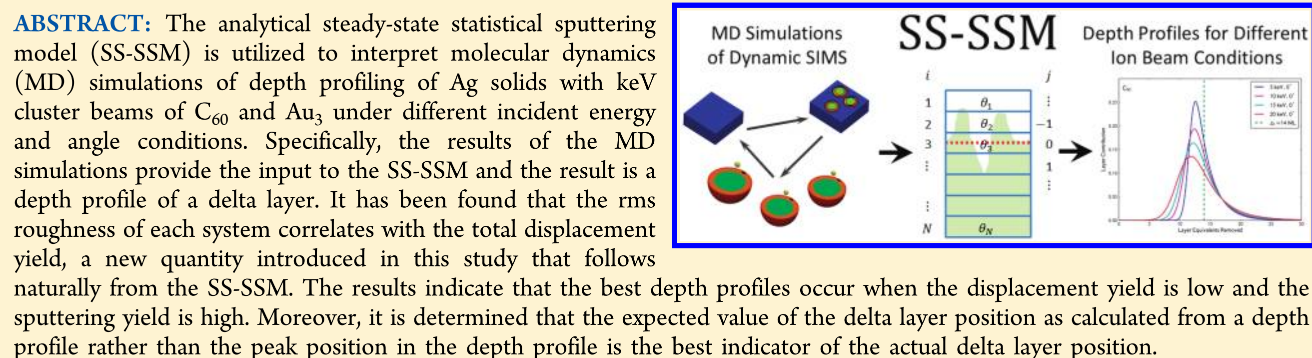

The introduction of cluster beams to the technique of secondary ion mass spectrometry (SIMS) has facilitated molecular depth profiling studies. Naturally, the community has turned their attention to determining the best conditions under which to perform the depth profiles. There are three basic types of cluster beams commercially available, small metal clusters such as Au_3[1] or Bi_3,[2] carbon based molecules such as buckyball,[3−5] and large clusters of Ar.[6] Each beam type has its proponents for the best cluster type. Not only must the optimal cluster type be chosen for a given experiment but also the optimal beam conditions. The most extensive studies of how beam parameters affect the depth profile have been performed for C_{60} bombardment of molecular solids. In general, lower beam energies give better depth profiles,[7−10] and more grazing angles of incidence give better depth profiles at an energy of 40 keV.[11−14] Issues may arise, however, if one combines these observations and selects low energy projectiles at an oblique incidence, for instance 10 keV C_{60} at 70°. One would expect that such condition would lead to the best depth profiles, an observation that is not confirmed experimentally.[15,16] Consequently, other factors, for instance a low sputtering yield, can be significant.[15,17] Sample rotation assists in improving the depth profile quality,[18,19] especially at grazing angles of incidence.[20] Sample cooling makes the depth profiles better for molecular solids[8,10,13,14,19,21,22] for reasons that are not yet understood although presumably tied to temperature activated chemical or electronic processes.

Concomitant with the experimental efforts, computational approaches are being brought to bear in order to understand depth profiling with cluster beams. A "divide and conquer" approach has been developed[23] to model with molecular dynamics (MD) simulations the removal of 3−4 nm equivalents of materials. These simulations have been performed for a number of beam conditions for an atomic solid, Ag(111).[23−26] Ongoing efforts are underway to perform analogous simulations on organic targets although these are very computationally intensive. In order to connect the MD results with experimental depth profiles, the statistical sputtering model (SSM)[27,28] and the steady-state SSM (SS-SSM)[29,30] have been developed. With these models, it is possible to extend the amount of material removed to any depth and thus to test general concepts of how beam conditions influence the depth profiles. Specifically, the SS-SSM predicts the depth profile of a delta layer.

The goal of this study is to apply the SS-SSM to the MD studies of C_{60} and Au_3 bombardment of Ag(111)[24,25] with varying beam conditions in order to elucidate on the atomic scale which bombardment characteristics have the largest influence on the quality of the depth profiles generated by the SS-SSM. The SS-SSM characterizes the sputtering and displacement distributions and connects them with a depth profile quality of a delta layer. The essential quantities in the model come from the steady-state region of the MD simulations. The distribution of number of atoms sputtered from each layer and the number of atoms displaced from one layer to another are the essential inputs to the SS-SSM. These quantities connect to the total sputtering yield and to a new quantity, the total displacement yield. The simulations analyzed here exhibit a direct relation between the ion beam induced roughness and the total displacement yield. This analysis also

Received: February 6, 2012
Accepted: February 24, 2012
Published: February 25, 2012

ACS Publications © 2012 American Chemical Society

leads to the conclusion that for the best depth profiles, one should minimize the displacement yield while maximizing the sputtering yield.

■ DESCRIPTION OF THE CALCULATIONS

The molecular dynamics (MD) simulations of repetitive bombardment (dynamic SIMS) of C_{60} and Au_3 using the "divide and conquer" protocol[23] have been reported previously.[24,25] The target system is Ag(111) with approximately five million atoms and a surface area of 2800 nm^2 (53 nm × 53 nm) for a computational cell with periodic boundary conditions. Several incident energies and incident angles were used for C_{60} and Au_3 bombardment of the system. The simulation starts with a perfectly flat surface, thus there is an induction period before the steady-state region is achieved as characterized by the rms roughness being relatively constant and the average surface level receding at a constant rate. Typically, 1500−2000 impacts for each set of beam conditions are calculated with approximately the latter half of the impact points being in the steady-state region. A simulation with 2000 impacts corresponds to a fluence of 7.3 × 10^{13} impacts/cm^2. The total time to execute a full simulation is approximately 4−5 months.

Details of the SS-SSM construction and prescription for evaluating the sputtering and displacements quantities from the MD results are given elsewhere.[29] In this paper, only a brief description is provided. The model is expressed by a set of differential equations for filling factors, i.e., fractional atom populations of system layers, as a function of amount of eroded material in monolayer (ML) units. Each differential equation contains three terms: a sputtering term describing the loss of atoms by sputtering, and two displacement terms describing the loss or gain of atoms by atom relocations to or from other layers. Special care is undertaken with the model formulation to prevent the unphysical behavior of layer overfilling. The model employs sputtering and displacement parameters for the differential equations as well as the average filling factors as the initial condition. These quantities are determined as averages relative to the average surface level over all the impacts within the steady-state region of the MD simulation. The layers used by the model are arbitrary and do not have to be directly associated with the monatomic layers of the original undisturbed system. The selected layer width is a compromise between the spatial resolution and the statistical noise of sputtering and displacement distributions calculated from MD data.[29] In the results presented here, we use a layer thickness of four monatomic Ag(111) layers or 0.94 nm which is approximately 1 nm. Thus, plots that have monolayer equivalents as a unit can be thought of as dimensions of nanometers. The delta layer width is the same as the monolayer width in the model, that is, approximately 1 nm.

The key connection between the MD simulations and the SS-SSM quantities is the evaluation of the sputtering, Γ_j, and the displacement, $\Delta_{j\to j'}$, terms. The sputtering parameter in its raw form Γ_j denotes the average number of atoms sputtered from the jth system layer per impact, where $j = 0$ represents the average surface level and $j < 0$ and $j > 0$ represent the layers above and below the average surface level, respectively. The displacement parameter $\Delta_{j\to j'}$ denotes the average number of atoms relocated from the jth to the j'th system layer per impact. Naturally, the sum of Γ_j over all j values yields the total sputtering yield in dynamic conditions. As a new concept arising from the SS-SSM, we also define the total displacement yield to be the sum of $\Delta_{j\to j'}$ over all j and j' values. We choose displacements between layers parallel to the original surface plane as we are interested in depth profiles. These displacements do not represent lateral motions that have also been observed in the simulations.[23,31,32] Whereas, the total sputtering yield is independent of the chosen layer thickness, the total displacement yield is not. For example, if the layer thickness is chosen sufficiently large, there will be no displacements between layers. Since the displacement yield is not uniquely defined, it cannot be measured experimentally. It does have utility, however, as a single quantity to use when discussing the amount of ion-beam induced mixing in the system per impact for different beam conditions.

Extracting depth profiles of delta layers requires tracking the fate of atoms originating from the initial system layers independently as described previously.[27,29] Because of the computational protocol of discrete shifting the average surface layer as material is removed, the depth profiles are jagged. In order to obtain smooth depth profiles as well as for quantitative purposes of determining the numerical characteristics of the depth profiles, the depth profile is fitted to the Dowsett's analytical response function (ARF),[10,33] which is typically used in experimental data analysis. As noted previously,[29] the integral of both the jagged depth profile and the fitted function is unity, thus correctly describing the removal of 1 ML from the system. The two quantities that are used from the fitted depth profile for comparison among the different beam conditions are the apparent delta-layer position and the full width half-maximum (fwhm) of the distribution. Which distance best represents the delta-layer position is also assessed.

■ RESULTS

The total sputtering yields, displacement yields, and rms roughness values for the 10 dynamic SIMS MD simulations are shown in Figure 1. Of note is that all of these are steady-state quantities and not for flat surface values. Depending on the beam conditions, the difference between values obtained on flat and roughened surfaces can be significant, especially for grazing angles of incidence.[24] The values of the quantities are given in Table 1. The sputtering yields shown in Figure 1a,b increase with increasing energy for both projectiles and decrease as the angle becomes more grazing for C_{60}. The impact angle behavior of Au_3 is different as small clusters deposit their primary energy relatively deep. As a result they have angle dependence resembling the one observed for atomic projectiles.[24] As found previously in a combined computational and experimental study of the yields for water ice,[34] the yields for C_{60} are larger than for Au_3 bombardment at the same beam conditions, although the difference decreases with the increase of the impact angle. The displacement yields shown in Figure 1c,d exhibit similar trends as the sputtering yields, increasing with energy and decreasing as the angle becomes more grazing. In contrast to the sputtering yields, the displacement yields are larger for Au_3 than for C_{60} bombardment for each set of beam conditions. This observation is consistent with the longer range of penetration of the Au_3 cluster than the C_{60} cluster.[34−36] For the chosen layer thickness of ∼1 nm, the ratio of the sputtering yield to displacement yield as given in Table 1 ranges from 0.04 to 0.23. Finally, the rms roughness values shown in Figure 1e,f exhibit similar trends as the sputtering and displacement yields, increasing with energy and decreasing as the angle becomes more grazing. As for displacement yields, the rms roughness is larger for Au_3 than for C_{60}.

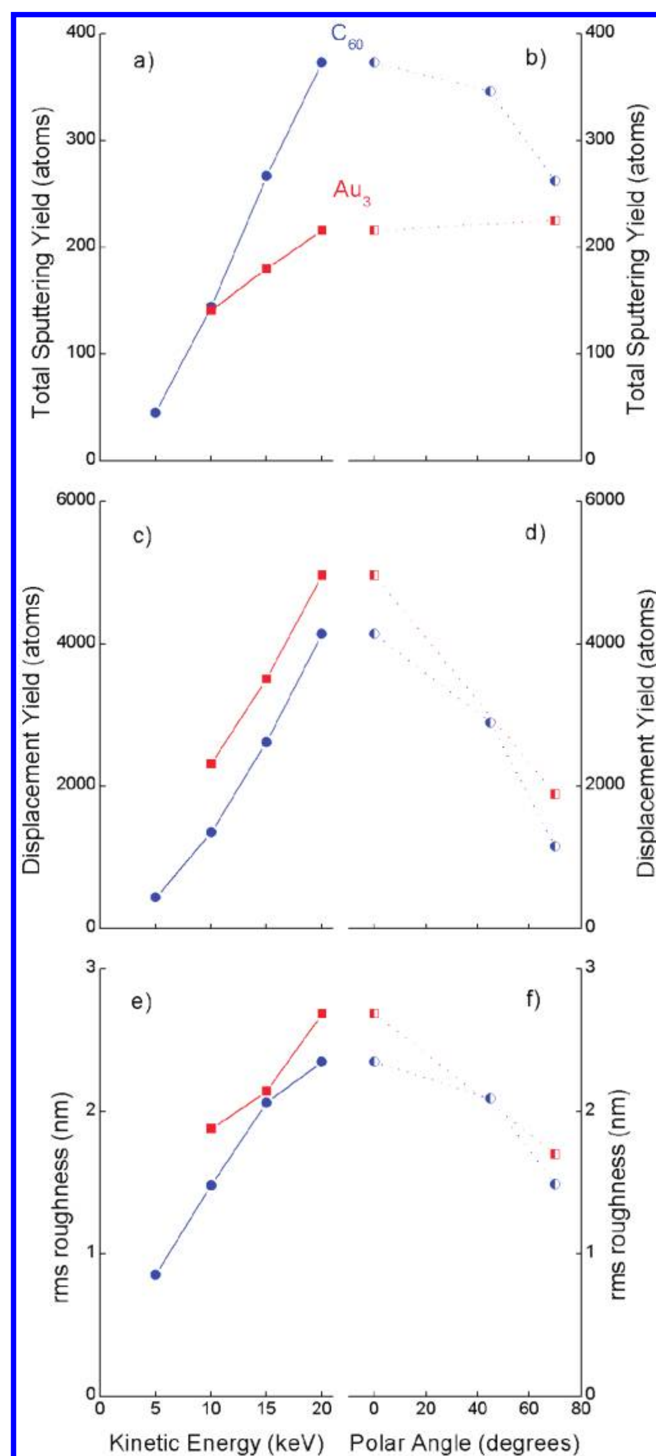

Figure 1. Total sputtering yield, displacement yield and rms roughness vs incident beam energy and angle. Results for C_{60} bombardment are shown in blue circles and for Au_3 bombardment in red squares. The angle dependent studies have half-filled symbols and dashed lines. All the kinetic energy simulations are for bombardment normal to the surface and all the angle dependent studies are for 20 keV incidence.

The depth profiles for delta-layer number 14 as calculated by the SS-SSM are shown in Figure 2 for all 10 simulations. General descriptions of how the SSM and SS-SSM model quantities affect the depth profiles are given elsewhere.[27−29] Here we focus on interpreting the results of the MD simulations. The depth profiles for different incident kinetic energies for C_{60} and Au_3 bombardment are shown in parts a and b of Figure 2, respectively. The better depth profiles are ones whose peak position is closest to layer 14 (vertical dashed green line) and whose fwhm is the smallest. By these measures, lowering the incident energy creates better depth profiles at normal incidence. This observation is in agreement with experimental data on molecular solids.[7−10] The depth profiles corresponding to changing the incident polar angle with a kinetic energy of 20 keV for C_{60} and Au_3 bombardment are shown in parts c and d of Figure 2, respectively. Changing the incident angle to more grazing improves the depth profile quality, again, an observation made by experiment on molecular solids.[11,13,37,38] In general, there is a correlation that the smaller the rms roughness value, the better the depth profile quality as measured by the peak position and the fwhm as shown in Figure 2 and Table 2. This conclusion is, however, not perfect. For instance, better depth profiles can be obtained for C_{60} bombardment at 20 keV and 70° than for 5 keV normal bombardment although 5 keV C_{60} normal incidence leads to much smaller rms roughness.[30]

The results from the SS-SSM provide the opportunity to assess what distance measure best reflects the actual delta layer position. There are four potential quantities. The easiest distance to see from the depth profile is the peak position. Another distance is the center of the Gaussian in the Dowsett fit. If the depth profile $\mathrm{ARF}(x)$ is considered as a statistical distribution, then there are two other distances, the median distance at which half of the delta layer has been removed and the expected value of the delta layer position as calculated from a depth profile, $\langle x \rangle$, where $\langle x \rangle = \int x\, \mathrm{ARF}(x)\, \mathrm{d}x / \int \mathrm{ARF}(x)\, \mathrm{d}x$. Two sets of values are given in Table 2, the peak position and the expected value of the delta layer position. Comparing only these two quantities, the expected value of the delta layer position is closer to the actual delta layer position and shows the least fluctuation with incident beam conditions. In fact, the expected value of the delta layer position is within one monolayer of the actual position. The values of the center of the Gaussian in the Dowsett fit are farther from the delta layer position than the peak position and the median distance is midway between the peak position and the expected value of the delta layer position. Thus, from these model calculations we conclude that the best distance to use for describing the delta layer position is the expected value of the delta layer position as calculated from a depth profile. This distance was suggested in experimental studies on Irganox delta layers using general considerations but without evidence.[7]

Molecular dynamics simulations of dynamic SIMS afford us the opportunity to explore which aspect of the bombardment dynamics is most illustrative of the ultimate rms roughness. Ideally, it would be nice to be able to predict rms roughness for a set of conditions without extensive simulations. For large Ar cluster bombardment of Si, Aoki et al. correlated crater depth for bombardment on a flat surface with rms roughness.[39] We find a similar correlation for these studies if we limit ourselves to normal incidence bombardment. The correlation does not hold, however, for off-normal angles of incidence (not shown). The quantity that does correlate with the rms roughness in these studies, however, is the total displacement yield as shown in Figure 3a. The larger the displacement yield, the larger the rms roughness. Not discussed here are partially completed dynamic SIMS simulations using Ar_{872} clusters.[26] We have calculated the displacement yields and rms roughness values for these simulations and find that also in this case there is a

Table 1. Beam Conditions Used in the Simulations, Steady State rms Roughness, Total Sputtering Yield, Total Displacement Yield, and Ratio of the Sputtering Yield to the Displacement Yield for 0.94 nm Layers

cluster	energy/keV	angle/deg	rms/nm	sputtering yield/atoms	displacement yield/atoms	ratio sputtering to displacement
C_{60}	5	0	0.85	45	434	0.10
C_{60}	10	0	1.48	144	1350	0.11
C_{60}	15	0	2.06	267	2616	0.10
C_{60}	20	0	2.35	373	4137	0.09
C_{60}	20	45	2.09	346	2895	0.12
C_{60}	20	70	1.49	262	1150	0.23
Au_3	10	0	1.88	141	2313	0.06
Au_3	15	0	2.14	180	3506	0.05
Au_3	20	0	2.69	216	4963	0.04
Au_3	20	70	1.7	225	1885	0.12

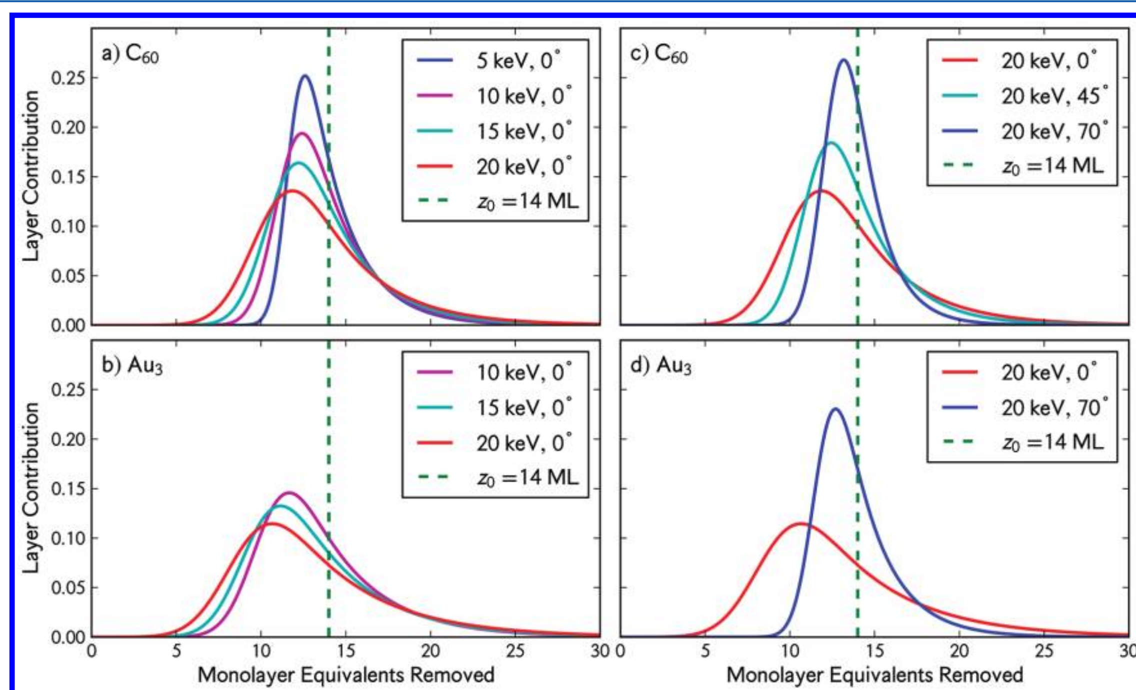

Figure 2. Depth profiles for all simulations. Each frame has a legend. The vertical green dashed line is the delta layer position.

Table 2. Parameters of the Dowsett Function That Fits the Depth Profiles Obtained from the SS-SSM[a]

cluster	energy/keV	angle/deg	λ_g/nm	σ/nm	λ_d/nm	peak position	$\langle x \rangle$	fwhm/nm
C_{60}	5	0	0.13	0.75	2.29	12.59	13.95	3.25
C_{60}	10	0	0.24	1.17	2.59	12.42	13.74	4.39
C_{60}	15	0	0.26	1.46	2.90	12.22	13.63	5.23
C_{60}	20	0	0.42	1.76	3.48	11.86	13.52	6.36
C_{60}	20	45	0.30	1.27	2.60	12.44	13.71	4.66
C_{60}	20	70	0.24	0.96	1.58	13.17	13.85	3.25
Au_3	10	0	0.37	1.49	3.57	11.66	13.54	5.83
Au_3	15	0	0.39	1.63	3.95	11.16	13.26	6.39
Au_3	20	0	0.33	1.89	4.62	10.66	13.14	7.39
Au_3	20	70	0.20	0.97	2.21	12.70	13.85	3.70

[a]The quantities λ_g, λ_d, and σ are the leading edge, trailing edge, and width quantities of the Dowsett function. The peak position of the distribution and the expected value of the delta layer position as calculated from a depth profile, $\langle x \rangle$, are also included.

monotonic correlation between these quantities although it is not the same as shown in Figure 3a. At this point, we do not know if there is a physical basis or whether it is fortuitous that the C_{60} and Au_3 data follow the same trend in Figure 3a. As stated above, the displacement yields depend on the chosen layer thickness so there is not necessarily any reason that the correlation for the different cluster beams should be similar. To summarize, the SS-SSM naturally leads to the definition of a total displacement yield per impact. We are proposing that the amount of displacement correlates with the amount of roughness that develops in depth profiling with dynamic SIMS. Further investigations will be performed to ascertain whether a better definition of displacements can be made in order to find an experimental test. To continue with the idea

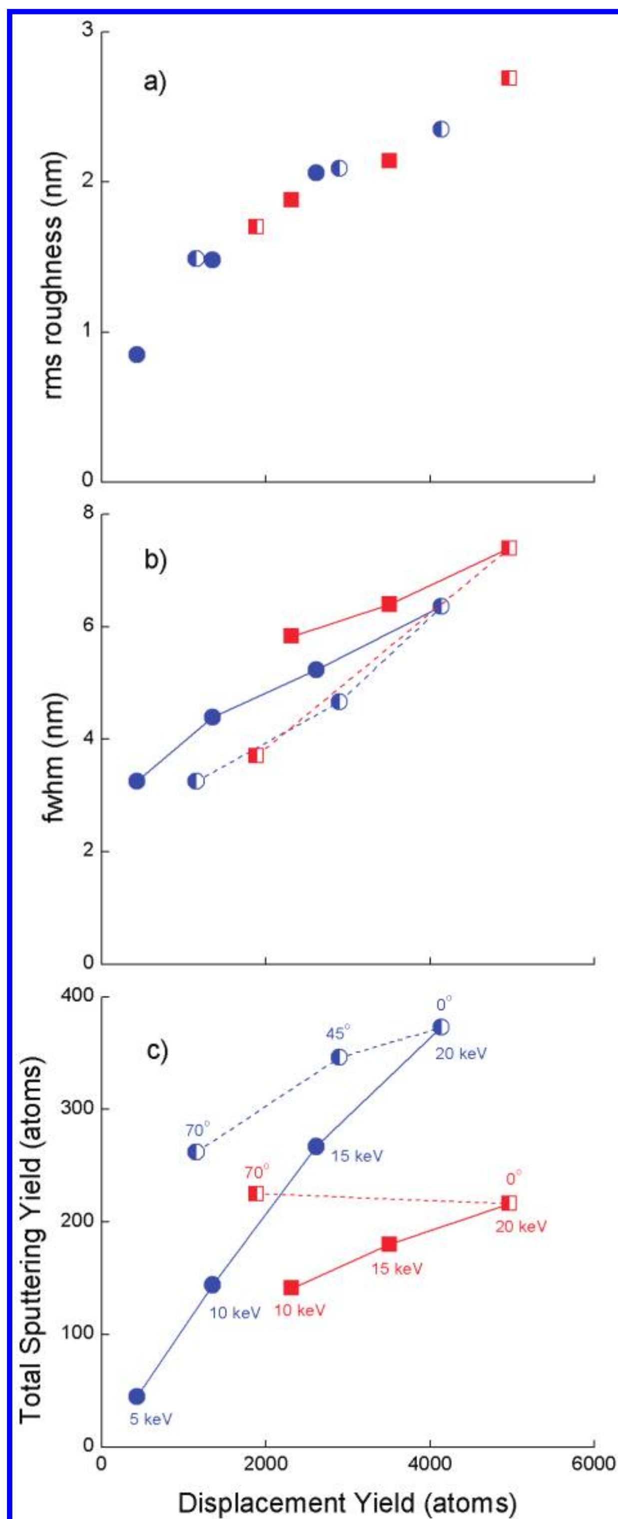

Figure 3. rms roughness, fwhm, and total sputtering yield vs displacement yield. Same color coding and line type are used as in Figure 1. The lines are guides to the eye to connect points and do not imply a specific dependence.

that the displacement yield is key, the fwhm and sputtering yield are shown versus displacement yield in parts b and c of Figure 3, respectively. Admittedly, these figures are compact. Pick one color for a cluster type, follow the solid line for the trend with kinetic energy at normal incidence and then the dashed line for the trend with an incident angle at 20 keV. For some clarity, the individual points are labeled in Figure 3c. For a given displacement yield, the fwhm values are smaller for C_{60} bombardment than Au_3 bombardment and smaller for grazing incidence than normal incidence. Correspondingly, for a given displacement yield, the sputtering yields are larger for C_{60} bombardment than Au_3 bombardment and greater for grazing incidence than normal incidence. These observations lead to a general conclusion that for the best depth profiles, one should increase the sputtering yield while keeping the displacement yield minimal.

To illustrate the nature of the dynamics that gives rise to these conclusions, the sputtering and displacement quantities that are input to the SS-SSM are given for four simulations as shown in Figure 4. The four simulations are C_{60} and Au_3, 20 keV incidence, at polar angles of 0° and 70°. The Γ and Δ distributions of Figure 4 contain considerable information about the behavior of the system. The sputtering yields per layer, Γ_j, are shown as vertical black bars. The peak of the distribution is approximately at the average surface level, $j = 0$. The width of the distribution is approximately ±2 × rms roughness which is given by the vertical green-dashed lines. The distributions tend to be skewed toward slightly more atoms being sputtered from above the average surface level ($j < 0$) rather than below the average surface level ($j > 0$). The displacement yields per layer, $\Delta_{j \to j'}$, are shown as lines for the various types of displacements as given in the figure legend. The displacement distributions for motion up and down one layer are more intense and broader than any other distribution including sputtering. The displacement distributions are broader than ±2 × rms roughness and tend to be skewed toward inside the solid. The fraction of atoms per layer that are not sputtered or displaced is given by the black dashed line that has approximately a sigmoidal shape.

The base system for the SS-SSM development[29] is C_{60} bombardment at 20 keV energy at normal incidence so we start with that distribution shown in Figure 4a. The sputttering yield is 0.09 times the displacement yield (Table 1), and the extent of the displacement distribution is well below the region from where sputtering occurs. Examining the change from C_{60} to Au_3 bombardment, the distributions for the same beam conditions are shown in Figure 4b. The displacement distributions are quite similar although the Au_3 ones are broader. The sputtering yield induced by Au_3, however, is smaller so that the ratio of the sputtering yield to the displacement yield is only 0.04, a value half that for C_{60} bombardment under the same conditions. Thus, even though these two beams produce a similar rms roughness, the sputtering yield for C_{60} bombardment is larger, thus it produces the better quality depth profile. Examining next the effect of angle of incidence, the Γ and Δ distributions for C_{60} and Au_3 bombardment at 20 keV and an angle of incidence of 70° are given in parts c and d of Figure 4, respectively. Compared to the normal angle bombardment, the sputtering yields for each beam are similar but the displacement yields diminish by about a factor of 3. Because of the reduced displacement yield at the grazing angle of incidence, the quality of the depth profile is better.

The most convincing support for this supposition comes from 5 keV C_{60} bombardment. As shown in Table 1, this condition gives rise to the smallest rms roughness and displacement yield. The Γ and Δ distributions for this system have been submitted for publication.[30] Although the rms roughness is small, the sputtering yield is also small. As a result,

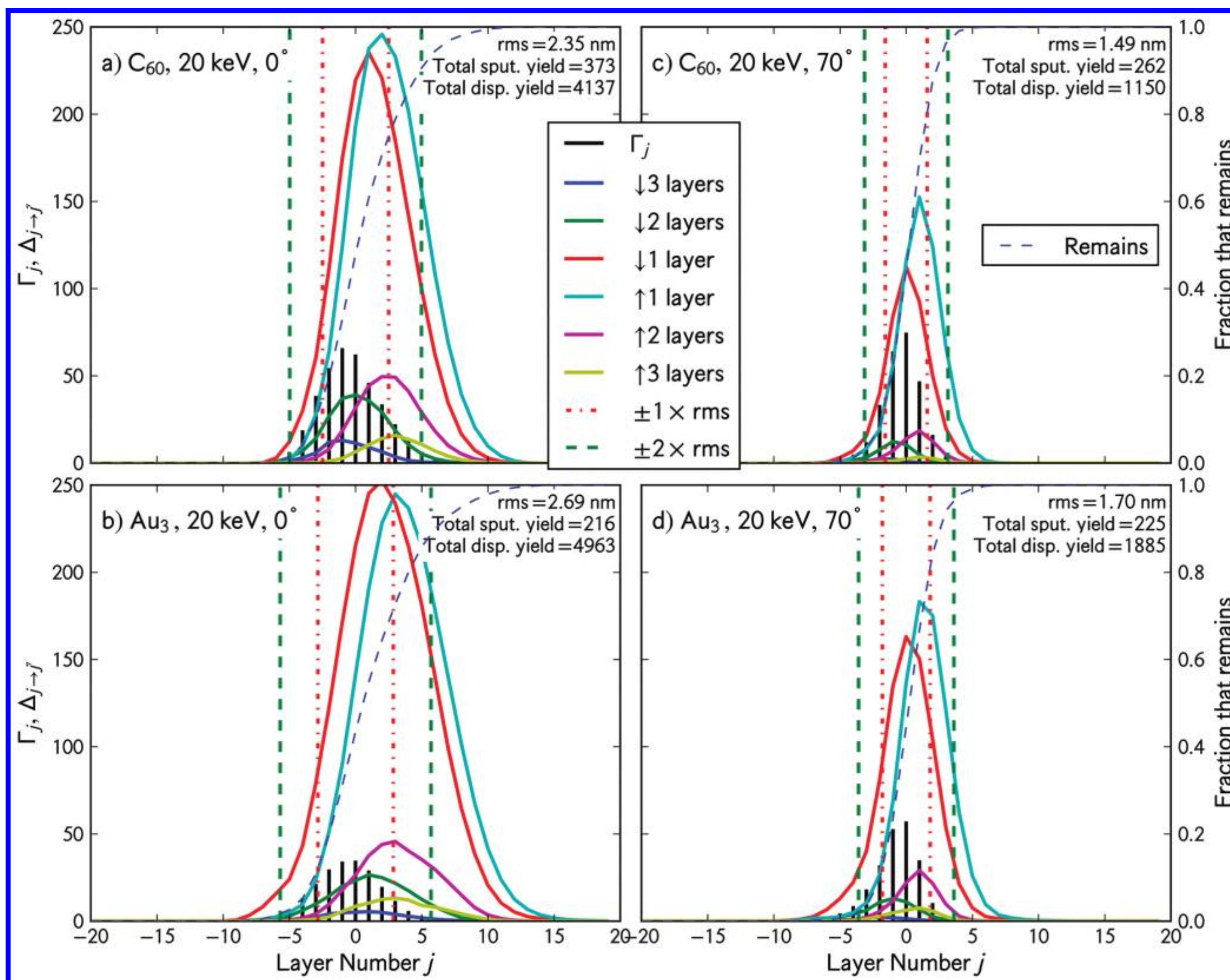

Figure 4. Average number of sputtered particles per layer, Γ_j, and average number of displaced particles per layer, $\Delta_{j \to j'}$, vs layer number, j. The sputtering yields are shown as vertical lines whereas the displacement yields are smooth lines with the color code defined in the legend. The red and green vertical lines correspond to ±1 and ±2 × rms roughness positions, respectively. The dashed blue line gives the fraction of a layer that remains in the layer and is not sputtered or displaced. (a) C_{60}, 20 keV, 0°; (b) Au_3, 20 keV, 0°; (c) C_{60}, 20 keV, 70°; (d) Au_3, 20 keV, 70°.

the ratio of the sputtering to displacement yields is small, and thus these conditions are not as good for depth profiling as C_{60} bombardment at 20 keV and 70° incidence where the sputtering yield is considerably higher. Increasing the sputtering yield is also important because it decreases the total time of the experiment.

The overall summary of the above discussion is that for good depth profiles, the ratio of the sputtering yield to displacement yield must be as large as possible. This statement is reminiscent of a simple model of molecular depth profiling proposed by Cheng, Wucher and Winograd.[40] Their model states that the total sputtering yield should be much greater than the damage created in the molecular system in order to attain molecular depth profiles, that is, a steady-state molecular signal as a function of fluence. Their model does not contain the concept of displacement of intact molecules. It will be interesting to assess the relative importance of molecular damage and intact molecular displacements on depth profile quality in ongoing MD simulations of dynamic SIMS of molecular organic targets.

■ CONCLUSIONS

Depth profiling of solids by energetic cluster beams is an important new process. Assessing the importance of various properties of the interaction of the cluster beam with the material on the depth profile quality is challenging. Using quantities from dynamic SIMS MD simulations partnered with the steady-state statistical sputtering model, we have correlated the rms roughness with the total displacement yield. Moreover, a simple concept has evolved that the best depth profiles emerge when the displacement yield is small and the sputtering yield is large. Moreover, it is determined that the expected value of the delta layer position as calculated from a depth profile rather than the peak position is the best indicator of the actual delta layer depth.

■ AUTHOR INFORMATION

Corresponding Author

*E-mail: bjg@psu.edu (B.J.G.); zbigniew.postawa@uj.edu.pl (Z.P.).

Notes

The authors declare no competing financial interest.

ACKNOWLEDGMENTS

The authors gratefully acknowledge financial support from the National Science Foundation Grant No. CHE-0910564 and the Polish National Science Center Programs No. PB1839/B/H03/2011/40 and PB 1247/B/H03/2010/39. We are extremely grateful to Andreas Wucher, Kristin Krantzman, and Alex Shard for helpful discussions.

REFERENCES

(1) Walker, A. V.; Winograd, N. *Appl. Surf. Sci.* **2003**, *203*, 198.
(2) Touboul, D.; Kollmer, F.; Niehuis, E.; Brunelle, A.; Laprevote, O. *J. Am. Soc. Mass Spectrom.* **2005**, *16*, 1608.
(3) VanStipdonk, M. J.; Harris, R. D.; Schweikert, E. A. *Rapid Commun. Mass Spectrom.* **1996**, *10*, 1987.
(4) Weibel, D.; Wong, S.; Lockyer, N.; Blenkinsopp, P.; Hill, R.; Vickerman, J. C. *Anal. Chem.* **2003**, *75*, 1754.
(5) Wong, S. C. C.; Hill, R.; Blenkinsopp, P.; Lockyer, N. P.; Weibel, D. E.; Vickerman, J. C. *Appl. Surf. Sci.* **2003**, *203*, 219.
(6) Ninomiya, S.; Ichiki, K.; Yamada, H.; Nakata, Y.; Seki, T.; Aoki, T.; Matsuo, J. *Rapid Commun. Mass Spectrom.* **2009**, *23*, 1601.
(7) Shard, A. G.; Green, F. M.; Brewer, P. J.; Seah, M. P.; Gilmore, I. S. *J. Phys. Chem. B* **2008**, *112*, 2596.
(8) Zheng, L. L.; Wucher, A.; Winograd, N. *Anal. Chem.* **2008**, *80*, 7363.
(9) Wucher, A.; Cheng, J.; Winograd, N. *J. Phys. Chem. C* **2008**, *112*, 16550.
(10) Lu, C. Y.; Wucher, A.; Winograd, N. *Anal. Chem.* **2011**, *83*, 351.
(11) Kozole, J.; Willingham, D.; Winograd, N. *Appl. Surf. Sci.* **2008**, *255*, 1068.
(12) Kozole, J.; Winograd, N. *Appl. Surf. Sci.* **2008**, *255*, 886.
(13) Kozole, J.; Wucher, A.; Winograd, N. *Anal. Chem.* **2008**, *80*, 5293.
(14) Mao, D.; Lu, C. Y.; Winograd, N.; Wucher, A. *Anal. Chem.* **2011**, *83*, 6410.
(15) You, Y. W.; Chang, H. Y.; Lin, W. C.; Kuo, C. H.; Lee, S. H.; Kao, W. L.; Yen, G. J.; Chang, C. J.; Liu, C. P.; Huang, C. C.; Liao, H. Y.; Shyue, J. J. *Rapid Commun. Mass Spectrom.* **2011**, *25*, 2897.
(16) Yu, B. Y.; Chen, Y. Y.; Wang, W. B.; Hsu, M. F.; Tsai, S. P.; Lin, W. C.; Lin, Y. C.; Jou, J. H.; Chu, C. W.; Shyue, J. J. *Anal. Chem.* **2008**, *80*, 3412.
(17) Schiffer, Z. J.; Kennedy, P. E.; Postawa, Z.; Garrison, B. J. *J. Phys. Chem. Lett.* **2011**, *2*, 2635.
(18) Rading, D.; Moellers, R.; Kollmer, F.; Paul, W.; Niehuis, E. *Surf. Interface Anal.* **2011**, *43*, 198.
(19) Sjovall, P.; Rading, D.; Ray, S.; Yang, L.; Shard, A. G. *J. Phys. Chem. B* **2010**, *114*, 769.
(20) Garrison, B. J.; Postawa, Z. *Chem. Phys. Lett.* **2011**, *506*, 129.
(21) Zheng, L. L.; Wucher, A.; Winograd, N. *Appl. Surf. Sci.* **2008**, *255*, 816.
(22) Mao, D.; Brenes, D. A.; Lu, C.; Wucher, A.; Winograd, N. *Surf. Interface Anal.* **2012**, submitted.
(23) Russo, M. F.; Postawa, Z.; Garrison, B. J. *J. Phys. Chem. C* **2009**, *113*, 3270.
(24) Paruch, R.; Rzeznik, L.; Russo, M. F.; Garrison, B. J.; Postawa, Z. *J. Phys. Chem. C* **2010**, *114*, 5532.
(25) Postawa, Z.; Rzeznik, L.; Paruch, R.; Russo, M. F.; Winograd, N.; Garrison, B. J. *Surf. Interface Anal.* **2011**, *43*, 12.
(26) Rzeznik, L.; Paruch, R.; Garrison, B. J.; Postawa, Z. *Nucl. Instrum. Methods Phys. Res., Sect. B* **2011**, *269*, 1586.
(27) Krantzman, K. D.; Wucher, A. *J. Phys. Chem. C* **2010**, *114*, 5480.
(28) Wucher, A.; Krantzman, K. D. *Surf. Interface Anal.* **2012**, submitted.
(29) Paruch, R. J.; Postawa, Z.; Wucher, A.; Garrison, B. J. *J. Phys. Chem. C* **2012**, *116*, 1042.
(30) Paruch, R. J.; Garrison, B. J.; Postawa, Z. *Surf. Interface Anal.* **2012**, submitted.
(31) Cook, E. L.; Krantzman, K. D.; Garrison, B. J. *Surf. Interface Anal.* **2012**, submitted.
(32) Krantzman, K. D.; Cook, E. L.; Wucher, A.; Garrison, B. J. *Nucl. Instrum. Methods Phys. Res., Sect. B* **2011**, *269*, 1591.
(33) Dowsett, M. G.; Rowlands, G.; Allen, P. N.; Barlow, R. D. *Surf. Interface Anal.* **1994**, *21*, 310.
(34) Russo, M. F.; Szakal, C.; Kozole, J.; Winograd, N.; Garrison, B. J. *Anal. Chem.* **2007**, *79*, 4493.
(35) Cheng, J.; Kozole, J.; Hengstebeck, R.; Winograd, N. *J. Am. Soc. Mass Spectrom.* **2007**, *18*, 406.
(36) Russo, M. F.; Garrison, B. J. *Anal. Chem.* **2006**, *78*, 7206.
(37) Ryan, K. E.; Garrison, B. J. *Anal. Chem.* **2008**, *80*, 5302.
(38) Ryan, K. E.; Smiley, E. J.; Winograd, N.; Garrison, B. J. *Appl. Surf. Sci.* **2008**, *255*, 844.
(39) Aoki, T.; Seki, T.; Matsuo, J. *Vacuum* **2010**, *84*, 994.
(40) Cheng, J.; Wucher, A.; Winograd, N. *J. Phys. Chem. B* **2006**, *110*, 8329.